Bioorganic & Medicinal Chemistry Letters 22 (2012) 2837–2842

Contents lists available at SciVerse ScienceDirect

Bioorganic & Medicinal Chemistry Letters

journal homepage: www.elsevier.com/locate/bmcl

Design and synthesis of 3-(4,5,6,7-tetrahydro-3*H*-imidazo[4,5-*c*]pyridin-2-yl)-1*H*-quinolin-2-ones as VEGFR-2 kinase inhibitors

Sun-Young Han [a,b], Jie Won Choi [a,c], Jeon Yang [a,d], Chong Hack Chae [a], Jongkook Lee [a], Heejung Jung [a], Kwangho Lee [a], Jae Du Ha [a,*], Hyoung Rae Kim [a], Sung Yun Cho [a,*]

[a] *Bio-Organic Science Division, Korea Research Institute of Chemical Technology, PO Box 107, Daejeon 305-600, Republic of Korea*
[b] *College of Pharmacy and Research Institute of Pharmaceutical Sciences, Gyeongsang National University, 816 Gil 15, Jinju-daero, Jinju, Gyeongnam 660-751, Republic of Korea*
[c] *Department of Chemistry, Sogang University, 1 Sinsoo-Dong, Mapo-Koo, Seoul 121-742, Republic of Korea*
[d] *Department of Chemistry, Chungnam National University, Yuseong, Daejeon 305-764, Republic of Korea*

ARTICLE INFO

Article history:
Received 2 December 2011
Revised 14 February 2012
Accepted 23 February 2012
Available online 7 March 2012

Keywords:
Cancer
VEGFR-2
KDR kinase
Imidazo[4,5-*c*]pyridine
Quinolin-2-one

ABSTRACT

A series of 3-(4,5,6,7-tetrahydro-3*H*-imidazo[4,5-*c*]pyridin-2-yl)-1*H*-quinolin-2-ones have been identified as a new class of VEGFR-2 kinase inhibitors. A variety of (4,5,6,7-tetrahydro-imidazo[5,4-*c*]pyridin-2-yl)-acetic acid ethyl esters were synthesized, and their VEGFR-2 inhibitory activity was evaluated. Described herein are the preparation of the series and the effects of the compounds on VEGFR-2 kinase activity.

Vascular endothelial growth factor receptor (VEGFR-2, KDR) is a receptor tyrosine kinase that plays important roles in regulating vascular permeability, endothelial cell proliferation and migration, and angiogenesis under physiological conditions mediated by vascular endothelial growth factor (VEGF).[1] Upon binding of the VEGF, VEGFR-2 dimerizes, autophosphorylates, and activates the VEGFR-2 pathway leading to angiogenesis, the formation of new capillaries from preexisting blood vessels, enhanced tumor survival, and tumor migration.[2] It has been postulated that the inhibition of angiogenesis by blocking the VEGFR-2 signaling pathway results in reduced tumor angiogenesis and tumor growth suppression.[3] Indeed, a number of inhibitors of VEGF-induced angiogenesis have been shown to be efficacious in tumor xenograft models.[4] Developing small-molecule VEGFR-2 inhibitors for anticancer therapy has been the goal of intensive drug discovery efforts at many pharmaceutical companies.[5] Sorafenib (Bayer/OSI)[6] and sunitinib (Pfizer),[7] are VEGFR-2 inhibitors that are used clinically against several types of cancer. Pazopanib (GlaxoSmithKline) and vandetanib (AstraZeneca) recently received FDA approval for renal cell carcinoma and medullary thyroid cancer, respectively (Fig. 1).

A variety of small-molecule inhibitors targeting VEGFR-2 have been reported and some of them have reached late-stage clinical development.[8] Described herein is a series of tetrahydro-3*H*-imidazo[4,5-*c*]pyridine-based inhibitors of VEGFR-2 that were substituted at the phenyl and tetrahydropyridine moieties. In our efforts to discover novel small-molecule VEGFR-2 kinase inhibitors, a class of compounds based on 3-(4,5,6,7-tetrahydro-3*H*-imidazo[4,5-*c*]pyridin-2-yl)-1*H*-quinolin-2-one (**1**) (Fig. 2) was identified. Compound **1** itself was identified as a hit with IC_{50} of 1 μM for the inhibition of VEGFR-2 kinase activity through high-throughput screening (HTS).

Owing to the structural similarities of **1** to known benzimidazolyl quinolinone **2** (IC_{50} of 1.7 μM)[9] and indolyl quinoxalinone **3** (IC_{50} of 8 nM)[10], both of which possessed submicromolar potency in the VEGFR-2 kinase assay, we sought to investigate the SAR in ring system A and at the nitrogen of the tetrahydropyridine with a focus on increasing intrinsic potency. In this communication, we report the development of tetrahydro-3*H*-imidazo[4,5-*c*]pyridine quinolinones as a new class of VEGFR-2 inhibitors.

According to the retrosynthetic analysis as shown in Scheme 1, the tetrahydro-3*H*-imidazo[4,5-*c*]pyridine quinolinones **1** could be readily prepared by condensing imidazopyridine acetates **5** with variously substituted 2-aminobenzaldehydes **4**. The corresponding imidazopiperidine acetates **5** were envisaged to come from the

* Corresponding authors. Tel.: +82 42 860 7077.
E-mail address: sycho@krict.re.kr (S.Y. Cho).

0960-894X/$ - see front matter © 2012 Elsevier Ltd. All rights reserved.
http://dx.doi.org/10.1016/j.bmcl.2012.02.073

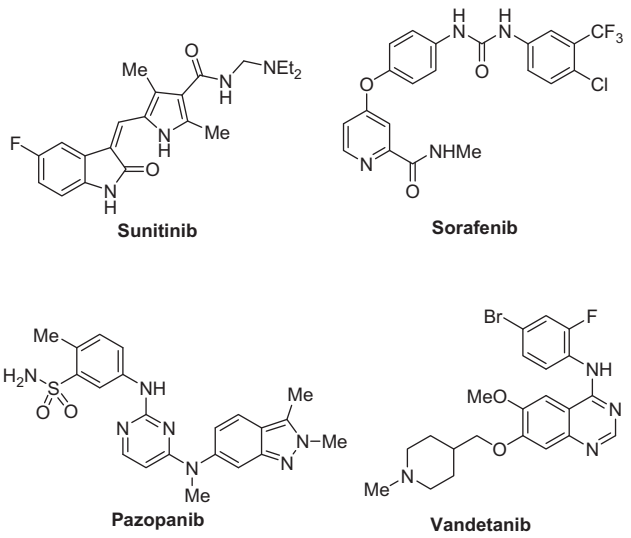

Figure 1. VEGFR-2 inhibitors approved.

condensation of imidate **6** with α-aminoketal derivatives **7**, which could be themselves prepared through a Neber rearrangement.[11]

As shown in Scheme 2, classical conditions for the synthesis of α-aminoketal derivatives **7** involved treatment of oxime tosylates **9** with KOEt. The tosylates were derived from various ketones **8** that were treated with hydroxylamine followed by tosylation of the corresponding oximes.

The preparation of imidazopiperidine acetates **5**[12] is outlined in Scheme 3. Imidazopiperidine **10** was reacted with suitable acyl halides to afford imidazopiperidine acetates **5**. A variety of N-substituted (4,5,6,7-tetrahydro-3*H*-imidazo[4,5-*c*]pyridin-2-yl)acetic acid ethyl ester derivatives were synthesized by following a known method (Scheme 4).[13]

Compounds were tested for VEGFR-2 inhibitory activity[14] and the results are summarized in Table 1. In the initial assessment, inhibitory activity in the micromolar range was observed with no substitution (**1**, **11**, **12**, **13**) on the phenyl group (ring A, R^2 = H) and simple alkyl or aryl substitutions at the imidazopiperidine nitrogen (R^1 = Me, Bn, methylpiperidine) on parent compound **1** Table 2.

Of the alkyl substituents, Cbz-protected piperidine (**12**) slightly improved inhibitory activity. N-substitution of the imidazopiperidine by either *meta*- (**14**, **15**) or *para*-nicotinamide (**17**, **18**) derivatives resulted in increased inhibitory activity. Introduction of fluorine at the 6-position of the phenyl ring significantly increased the inhibitory activity (**16**). 5-Fluorophenyl substitution did not significantly improve the activity of the *para*- and *meta*-nicotinamide derivatives (**15** and **18**, respectively). However, compound **19** containing a 6-F and *para*-nicotinamide exhibited picomolar inhibitory activity. To understand the SAR of N-substitution at the imidazopiperidine, we investigated substitutions with other amines, such as morpholine (**23**–**27**), piperazine (**28**–**32**), piperidine (**33**–**37**), and pyrrolidine (**38**). Introduction of a chlorine (**26**) at the C(6) position of the phenyl ring instead of fluorine (**25**) decreased potency. Interestingly, loss of activity was also observed with hydrogen at C(5) (**23**), fluorine at C(5) (**24**), and methoxy at the C(6) position (**27**) of the phenyl ring. Piperazine had a similar propensity to attenuate the potency of the compounds. Introduction of a chlorine (**31**) or methoxy group (**32**) in place of the fluorine (**30**) at the C(6) position of the phenyl ring decreased the inhibitory activities of the piperazine derivatives. Similar results were observed in the piperidine derivatives (**35**, **36**). Next, we tried to introduce a 3- or 4-pyridyl acetate in place of nicotinamide in the derivatives. Among these pyridyl acetates, 2-pyridyl acetate exhibited a high overall increase in potency with H or F at the

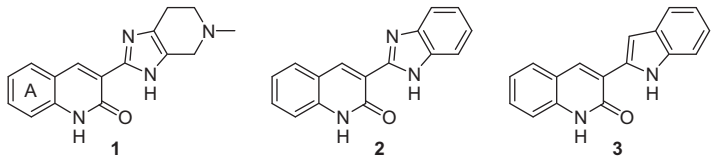

Figure 2. Structures of VEGFR-2 inhibitors **1**–**3**.

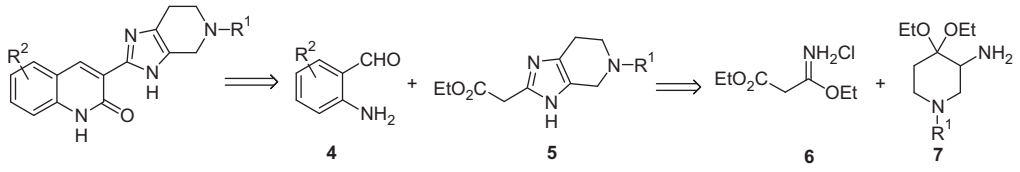

Scheme 1. Retrosynthetic analysis of tetrahydro-3*H*-imidazo[4,5-*c*]pyridine quinolinones.

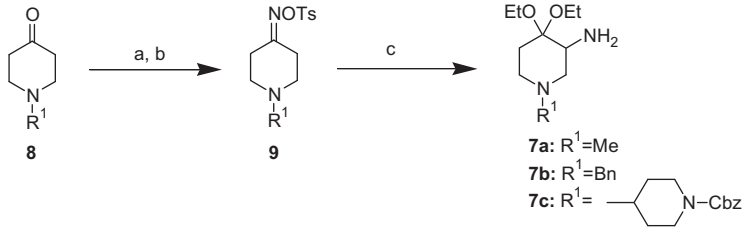

Scheme 2. Preparation of α-aminoketal derivatives **7** via a Neber rearrangement. Reagents and conditions: (a) NH_2OH, K_2CO_3, EtOH, reflux, 80–90%; (b) TsCl, pyridine, rt, 90%; (c) K, EtOH, Na_2SO_4, 60 °C, 40–90%.

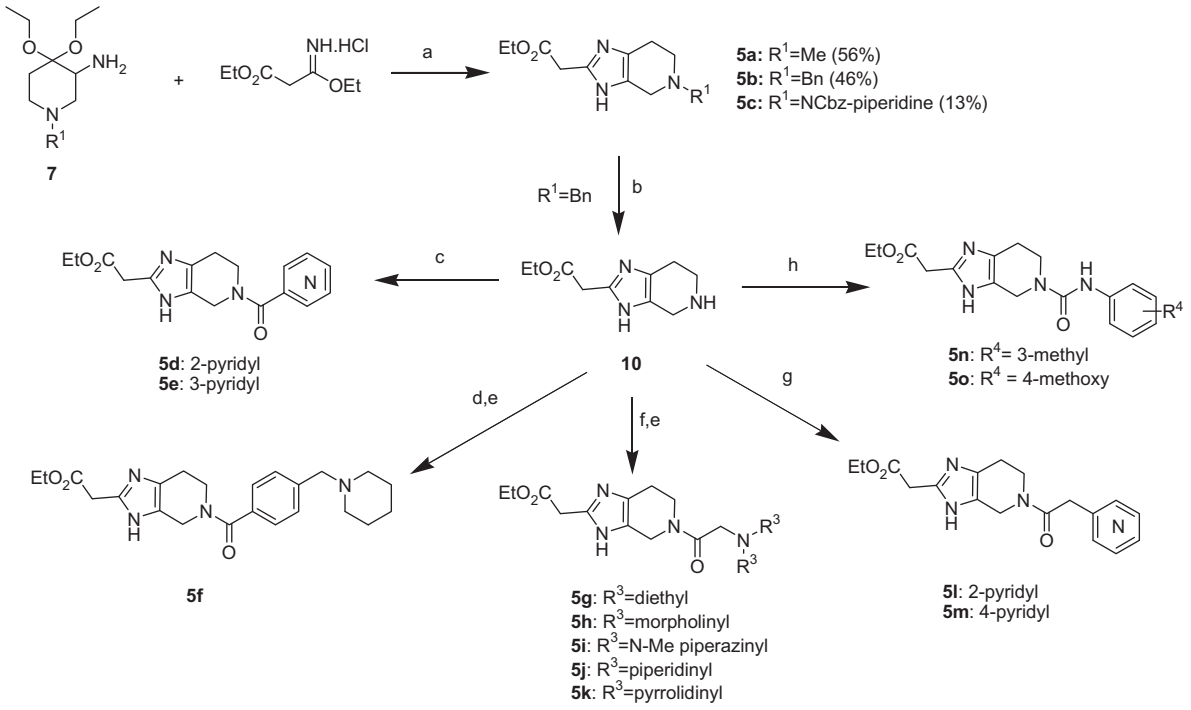

Scheme 3. Preparation of imidazopiperidine acetates **5**. Reagents and conditions: (a) 4 M-HCl/dioxane, EtOH, reflux, 72%; (b) $Pd(OH)_2$, EtOH, 60 psi, 92%; (c) pyridinecarboxylic acid, HOBT, EDCI, *N*-methylmorpholine, rt, 32–40%; (d) 4-chloromethylbenzoyl chloride, Et_3N, CH_2Cl_2, 0 °C, 62%; (e) amine, K_2CO_3, KI, THF, rt, 63%; (f) $ClCH_2COCl$, Et_3N, CH_2Cl_2, 0 °C, 42%; (g) pyridinylacetic acid, HOBT, EDCI, *N*-methylmorpholine, 40–50%; (h) isocyanates, CH_2Cl_2, rt, 55–62%.

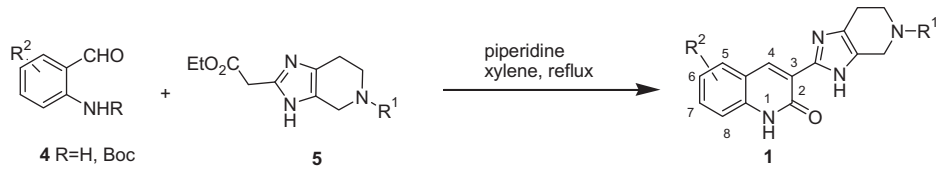

Scheme 4. Synthesis of tetrahydro-3*H*-imidazo[4,5-*c*]pyridine quinolinones.

C(6) position of the phenyl ring. When modifying the core with 4-pyridyl acetate, chlorine (**43**) at the C(6) position of the phenyl ring in place of H (**41**) or F (**42**) gave rise to inhibitory activity in the picomolar range.

Measurement of CYP (cytochrome P450) inhibitory activity and microsomal stability were performed to obtain a preliminary evaluation of the toxicities of selected compounds. The data revealed excellent microsomal stabilities and no significant CYP inhibitory activity except from compound **42** with respect to 2C9, 3A4 and 2D6. **19** and **21** inhibited 2C9 and 3A4, respectively.

The selected compounds were examined for their inhibitory activity on the proliferation of human umbilical vein endothelial cells (HUVEC) induced by the VEGF. The inhibitory activity of compounds on cell proliferation was measured using a Premix WST-1 cell proliferation assay kit.[18] In addition, the selected compounds were evaluated for inhibitory activity against HUVEC tube formation by Image-Pro Plus (Media Cybernetics) image analysis.[19] As shown in Table 3, selected compounds **19** and **21** showed weak inhibitory activity for HUVEC proliferation. Compound **19** exhibited marginal inhibitory activities for HUVEC tube formation at 10 μM and no activity was observed for **21** (data not shown). The low activities for HUVEC proliferation and tube formation of **19** and **21** was presumably attributed to the low degree of cell penetration (Table 4).

To provide a rational for the experimental in vitro activities of the quinolinone derivatives, compounds were docked into the crystal structure of VEGFR-2 (pdb code: 3VHE) by using the Glide software with standard precision (SP) protocols.[20] The representative binding mode of most active compound **19** was shown in Figure 3.

The quinolinone compounds fit tightly into the ATP binding cavity of the VEGFR-2 in inactive conformation with similar hydrogen bondings to Sutent in KIT kinase.[21] Hydrogen bonding interactions are observed between the carbonyl of the quinolinone ring and N of C919 in the hinge region (3.12 Å). The hydrogen bonding between the NH of the quinolinone and the main chain carbonyl of E917 is somewhat blocked by the collision of ring A with V916 and V899, and this may be the cause of low potency of this compounds. The fluorine at the C(6) position of ring A makes additional hydrogen bonding with NH of K868 (3.43 Å). Without this interaction, the potency is lowered as shown in series (Table 1, compounds (**14**–**19**), (**24**–**26**), (**28**–**30**), (**33**–**35**), and (**39**, **40**). The chlorine makes better interaction with K868 than methoxy group, as shown in series (Table 1, compounds **26**, **27**, **31**, **32**, **36**, **37**). The pyridinone ring stackes into the hydrophobic cleft comprised of A866, L1035 and C1045, and the piperidine ring makes hydrophobic interaction with the side chain of L840 and Cα of G922. The R^1 substituents extend into the solvent exposed region. The docking study indicated that the quinolinone compounds could fit into the binding site and could be potent VEGFR-2 inhibitors.

In summary, we identified a novel 3-(4,5,6,7-tetrahydro-3*H*-imidazo[4,5-c]pyridin-2-yl)-1*H*-quinolin-2-one scaffold that

Table 1
SAR of the 3-(4,5,6,7-tetrahydro-3*H*-imidazo[4,5-*c*]pyridin-2-yl)-1*H*-quinolin-2-one derivatives

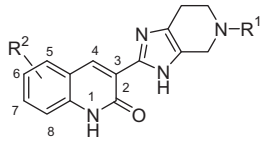

1

Compounds	R^1	R^2	VEGFR-2 IC_{50} (μM)	Compounds	R^1	R^2	VEGFR-2 IC_{50} (μM)[14]
1	Me	H	1	**28**	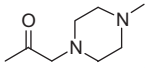	H	0.3
11	Bn	H	6	**29**	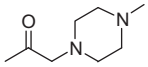	5-F	1.05
12	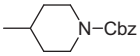	H	0.6	**30**	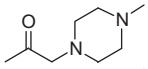	6-F	0.013
13	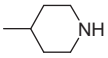	H	5	**31**	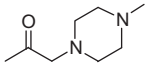	6-Cl	0.019
14	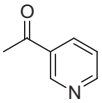	H	0.2	**32**	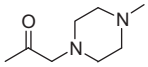	6-OMe	1.1
15	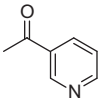	5-F	0.6	**33**	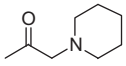	H	0.016
16	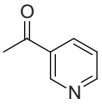	6-F	0.001	**34**	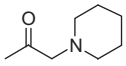	5-F	0.74
17	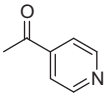	H	0.2	**35**	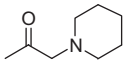	6-F	0.008
18	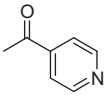	5-F	0.8	**36**	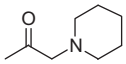	6-Cl	0.022
19	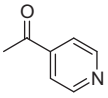	6-F	0.0003	**37**	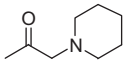	6-OMe	0.28
20	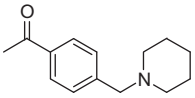	H	0.0013	**38**	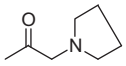	H	0.4
21	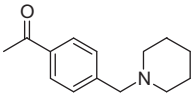	6-F	0.0049	**39**	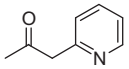	H	0.0013
22	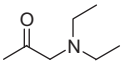	H	0.3	**40**	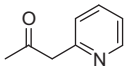	6-F	0.0007
23	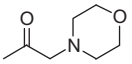	H	0.3	**41**	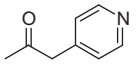	H	0.0067
24	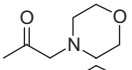	5-F	1.1	**42**	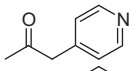	6-F	0.0086
25	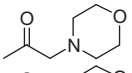	6-F	0.0043	**43**	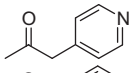	6-Cl	0.0005
26	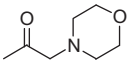	6-Cl	0.035	**44**	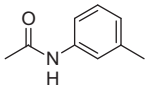	H	0.0021
27	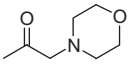	6-OMe	0.76	**45**	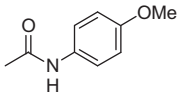	H	0.046

Table 2
Effects of compounds **19** and **21** on CYP inhibitory activity and microsomal stability

	CYP (% remaining activity at 10 μM)[15]					Microsomal stability (% remaining activity at 10 μM; 30 min incubation)[16]	Permeability[17] (PAMPA)
	1A2	3A4	2C9	2C9	2D6	Human	nt[a]
16	86	83	99	92	67	96	nt
19	96	89	53	77	90	99	−6.2
21	89	16	94	100	100	92	−6.8
42	58	33	28	35	21	93	nt

[a] Not tested.

Table 3
Results of VEGF-induced HUVEC anti-proliferative activity[18] for **19** and **21**

Control	VEGF (20 ng/ml)	VEGF + compound **19**			VEGF + compound **21**		
		0.1 μM	1 μM	10 μM	0.1 μM	1 μM	10 μM
100	179	120	72	71	92.3	82	79

Table 4
Effects of compound **19** and **21** on HUVEC tube formation (% of control)[19]

Control	Compound **19**		Compound **21**	
	1 μM	10 μM	1 μM	10 μM
100	93	62	102	99

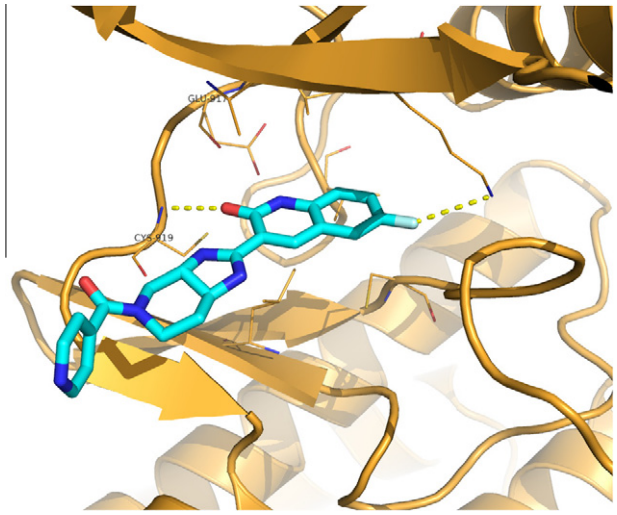

Figure 3. Docking model of VEGFR-2 with compound **19**. The side chains of binding site are shown as lines and labeled with their residue name. Hydrogen bondings are shown in yellow dashed lines. Parts of the P-loop residues are omitted for clarity.

exhibited potent VEGFR-2 inhibitory activity. Compounds **19** and **21** had marginal inhibitory activities for HUVEC proliferation and tube formation with stable microsomal stabilities and low degrees of binding to CYPs. Introduction of F and Cl at the C(6) position of the phenyl ring dramatically increased VEGFR-2 inhibitory activity.

Acknowledgments

This work was supported in part by a Grant for the anti-cancer research program from the Korea Research Institute of Chemical Technology (KRICT) and the Basic Science Research Program from NRF (2011-0010374, S.-Y.H.) funded by the government of Korea (MEST). We thank the Drug Discovery Technology Platform team at KRICT for providing us with technical assistance on the CYP activity and microsomal stability experiments.

References and notes

1. (a) Olsson, A. K.; Kimberg, A.; Kreuger, J.; Claesson-Welsh, L. *Nat. Rev. Mol. Cell Biol.* **2006**, *7*, 359; (b) Ferrara, N.; Gerber, H.; LeCouter, J. *Nat. Med.* **2003**, *9*, 669; (c) Carmeliet, P. *Nat. Med.* **2003**, *9*, 653–660; (d) Yang, J. C.; Haworth, L.; Sherry, R. M.; Hwu, P.; Schwartzentruber, D. J.; Topalian, S. L.; Steinberg, S. M.; Chen, H. X.; Rosenberg, S. A. *N. Eng. J. Med.* **2003**, *349*, 427.
2. Ferrara, N.; Gerber, H.; LeCouter, J. *Nat. Med.* **2003**, *6*, 669.
3. (a) Cross, M. J.; Claesson-Welsh, L. *Trends Pharmacol. Sci.* **2001**, *22*, 201; (b) McMahon, G. *Oncologist* **2000**, *5*, 3; (c) Prewett, M.; Huber, J.; Li, Y.; Santiago, A.; O'Connor, W.; King, K.; Overholser, J.; Hooper, A.; Pytowski, B.; Witte, L.; Bohlen, P.; Hicklin, D. J. *Cancer Res.* **1999**, *59*, 5209.
4. (a) Cohen, M. H.; Gootenberg, J.; Keegan, P.; Pazdur, R. *Oncologist* **2007**, *12*, 356; (b) Sandler, A.; Gray, R.; Perry, M. C.; Brahmer, J.; Schiller, J. H.; Dowlati, A.; Lilenbaum, R.; Johnson, D. H. *N. Eng. J. Med.* **2006**, *355*, 2542; (c) Cardones, A. R.; Banez, L. L. *Curr. Pharm. Des.* **2006**, *12*, 387.
5. (a) Boyer, S. J. *Curr. Top. Med. Chem.* **2002**, *2*, 973; (b) Traxler, P. *Expert Opin. Ther. Targets* **2003**, *2*, 215.
6. (a) Atkins, M.; Jones, C. A.; Kirkpatrick, P. *Nat. Rev. Drug Disc.* **2006**, *5*(4), 279–280; (b) Strumberg, D. *Drugs Today* **2005**, *41*, 773.
7. Ng, R.; Chen, E. X. *Curr. Clin. Pharmacol.* **2006**, *1*, 223–228.
8. (a) Rosen, L. S.; Kurzrock, R.; Mulay, M.; Van Vugt, A.; Purdom, M.; Ng, C.; Silverman, J.; Koutsoukos, A.; Sun, Y.-N.; Bass, M. B.; Xu, R. Y.; Polverino, A.; Wiezorek, J. S.; Chang, D. D.; Benjamin, R.; Herbst, R. S. *J. Clin. Oncol.* **2007**, *25*(17), 2369; (b) Harmange, J.; Weiss, M.; Germain, J.; Polverino, A. J.; Borg, G.; Bready, J.; Buckner, W.; Chen, D.; Choquette, D.; Coxon, A.; DeMelfi, T.; DiPietro, L.; Doerr, N.; Estrada, J.; Fellows, I.; Flynn, J.; Graceffa, R. F.; Harriman, S. P.; Kaufman, S.; La, D. S.; Long, A.; Martin, M. W.; Neervannan, S.; Patel, V. F.; Potashman, M.; Regal, K.; Roveto, P. M.; Schrag, M. L.; Starnes, C.; Tasker, A.; Teffera, Y.; Wang, L.; White, R. D.; Whittington, D.; Zanon, R. *J. Med. Chem.* **2008**, *51*, 1649; (c) Weiss, M. M.; Harmange, J.; Polverino, A. J.; Bauer, D.; Berry, L.; Berry, V.; Borg, G.; Bready, J.; Bretz, A.; Chen, D.; Chi, V.; Choquette, D.; Coxon, A.; DeMelfi, T.; Doerr, N.; Estrada, J.; Fellows, I.; Flynn, J.; Graceffa, R. F.; Harriman, S. P.; Kaufman, S.; La, D. S.; Long, A.; Neervannan, S.; Patel, V. F.; Potashman, M.; Regal, K.; Roveto, P. M.; Schrag, M. L.; Starnes, C.; Tasker, A.; Teffera, Y.; Whittington, D.; Zanon, R. *J. Med. Chem.* **2008**, *51*, 1668–1680; (d) Mendel, D.; Laird, D.; Xin, X.; Louie, S.; Christensen, J.; Li, G.; Schreck, R.; Abrams, T.; Ngai, T.; Lee, L.; Murray, L.; Carver, J.; Chan, E.; Moss, K.; Haznedar, J.; Sukbuntherng, J.; Blake, R.; Sun, L.; Tang, C.; Miller, T.; Shirazian, S.; McMahon, G.; Cherrington, J. *Clin. Cancer Res.* **2003**, *9*, 327.
9. Renhowe, P. A.; Pecchi, S.; Shafer, C. M.; Machajewski, T. D.; Jazan, E. M.; Taylor, C.; Antonios-McCrea, W.; McBride, C. M.; Frazier, K.; Wiesmann, M.; Lapointe, G. R.; Feucht, P. H.; Warne, R. L.; Heise, C. C.; Menezes, D.; Aardalen, K.; Ye, H.; He, M.; Le, V.; Vora, J.; Jansen, J. M.; Wernette-Hammond, M. E.; Harris, A. L. *J. Med. Chem.* **2009**, *52*, 278.
10. Fraley, M. E.; Arrington, K. L.; Buser, C. A.; Ciecko, P. A.; Coll, K. E.; Fernandes, C.; Hartman, G. D.; Hoffman, W. F.; Lynch, J. J.; McFall, R. C.; Rickert, K.; Singh, R.; Smith, S.; Thomas, K. A.; Wong, B. K. *Bioorg. Med. Chem. Lett.* **2004**, *14*, 351.
11. (a) Neber, P. W.; Burgard, A.; Their, W. *Ann. Chem.* **1936**, *1*, 277; (b) LaMattina, J. L.; Suleske, R. T. *Synthesis* **1980**, *1*, 329; (c) LaMattina, J. L.; Sulske, R. T. *Org. Synth.* **1986**, *64*, 19; (d) Itoh, K.; Oka, Y. *Chem. Pharm. Bull.* **1983**, *2016*, 31; (e) Diez, A.; Voldoire, A.; Lopez, I.; Rubiralta, M.; Segarra, V.; Pages, L.; Palacios, J. M. *Tetrahedron* **1995**, *51*, 5143.
12. Ha, J. D.; Lee, S. J.; Nam, S. Y.; Kang, S. K.; Cho, S. Y.; Ahn, J. H.; Choi, J.-K. *Tetrahedron Lett.* **2006**, *47*, 6201.

13. For the reaction between 2-benzoimidazole-2-ylacetate and 2-aminobenzaldehyde: Fraley, M. E.; Hambaugh, S. R.; Hungate, R. W. U.S. Patent 6479512 B1, 2002.
14. *VEGFR-2 kinase assay*: Inhibition of kinase activity against recombinant VEGFR-2 protein was measured using homogeneous time-resolved fluorescence (HTRF) assays. Recombinant proteins containing VEGFR-2 kinase domain were purchased from Millipore. Optimal enzyme, ATP, and substrate concentrations were established using HTRF KinEASE kit (Cisbio) according to the manufacturer's instructions. Assays are composed of the VEGFR-2 enzyme mixed with serially diluted compounds and peptide substrates in a kinase reaction buffer (250 mM HEPES (pH 7.0), 0.5 mM orthovanadate, 0.05% BSA, 0.1% NaN_3, 5 mM $MgCl_2$, 1 mM $MnCl_2$, 1 mM DTT, supplement enzymatic buffer). Following the addition of reagents for detection, the Time Resolved-Fluorescence Resonance Energy Transfer (TR-FRET) signal was measured using an EnVision multi-label reader (Perkin Elmer). Dose–response curves were generated to determine IC_{50} using Prism version 5.01 (GraphPad).
15. *CYP450 inhibition assay*: The potential of **21** to inhibit major human cytochrome P450 (CYP450) enzymes was evaluated using a recombinant CYP450 inhibition kit (Invitrogen Vivid). The IC_{50} values of **21** for each CYP isoform was determined from the inhibition of major five CYP450 isoform such as CYP1A2, CYP2C9, CYP2C19, CYP2D6, and CYP3A4 by fluorescence detection in 96-well format. The studies were conducted in duplicate over a 20 min incubation period with 20 min pre-incubation at room temperature. The IC_{50} values were estimated using Prism Software.
16. *Microsomal stability test*: NADPH dependent oxidative metabolism of **21** in human and rat liver microsomes was determined on single-time-point 30 min. The reaction mixtures consisted of human or rat liver microsomes (0.5 mg/ml; BD Gentest) in 100 mM potassium phosphate buffer (pH 7.4) and final concentration of **21** was 2 μM. After pre-incubation of reaction mixture at 37 °C for 5 min, the reaction was initiated by addition NADPH regeneration solution (BD Biosciences) and the reaction was terminated by adding three times volume of ice-cold acetonitrile with imipramine (80 ng/ml) as internal standard at single-time-point 30 min. After pretreatment of biological samples with vortex and centrifuging, the samples were analyzed by LC/MS/MS system (AB Sciex 2000 Qtrap).
17. Ottaviani, G.; Martel, S.; Carrupt, P.-A. *J. Med. Chem.* **2006**, *49*, 3948.
18. *In vitro VEGF-induced HUVEC proliferation assay*: Pooled HUVECs (Lonza) were grown in a 1:1 mixture of EBM-2 medium with EGM-2 supplements and used at passage eight or lower. HUVECs were placed at a density of 10,000 cells/well on a collagen type I precoated 96-well plate. After 24 h, the cells were incubated for 24 h in the presence of rhVEGF (20 ng/mL) in the presence of the compound under examination. Cells were assayed for proliferation by the Premix WST-1 proliferation assay system (Takara).
19. *In vitro angiogenesis assay (tube formation)*: 24-well plates were coated with 200 mL of a 1:1 mixture of Matrigel (10 mg/mL) and EBM-2 medium with EGM-2 supplements and incubated at 37 °C for 1 h. HUVECs (Lonza) were placed at a density of 40,000/well and incubated for 16–18 h. After incubation, the plates were fixed and images were captured using a Nikon camera (50×) and analyzed using Image-Pro Plus software (Media Cybernetics).
20. Friesner, R. A.; Banks, J. L.; Murphy, R. B.; Halgren, T. A.; Klicic, J. J.; Mainz, D. T. *J. Med. Chem.* **2004**, *47*, 1739.
21. Gajiwala, K. S.; Wu, J. C.; Christensen, J.; Deshmukh, G. D.; Diehl, W.; DiNitto, J. P.; English, J. M.; Greig, M. J.; He, Y. A.; Jacques, S. L.; Lunney, E. A.; McTigue, M.; Molina, D.; Quenzer, T.; Wells, P. A.; Yu, X.; Zhang, Y.; Zou, A.; Emmett, M. R.; Marshall, A. G.; Zhang, H. M.; Demetri, G. D. *Proc. Natl. Acad. Sci. U.S.A.* **2009**, *106*, 1542.